Chapter 1: Introduction

1.1 Nonlinear dynamics in electrochemistry

The occurrence of dynamic instabilities, *e.g.*, bistable or oscillatory behavior, in electrochemical systems is a wide-spread phenomenon. In fact, it can be expected to occur under certain conditions in nearly every electrochemical reaction. Since the first observations of oscillations during metal dissolution in 1828 [1], a large variety of dynamic behavior has been discovered in many electrochemical reactions [2, 3].

In the early days, research concentrated on metal dissolution reactions, in which also the concept of the development of spatial structures was introduced [4-9]. It became apparent that the observed oscillations were often accompanied or caused by pulse propagation in the potential drop between electrode and electrolyte; the simultaneous removal and consequent formation of an oxide film after the passage of the pulse on the electrode was optically easy to detect. These potential pulses were soon also considered as inorganic model systems to understand and study the electrophysiological pattern formation of potential pulses travelling along axons to transport neural excitation. However, this major motivation to investigate electrochemical pattern formation ceased considerably after the development of the patch-clamp-method [10] which made it possible to conduct quantitative experiments on real biological axons.

In the last decade, a renewed interest in electrochemical pattern formation has been seen since the observation of inhomogeneous oscillations during the dissolution of nickel in 1988 [11]. As a result of the development of micro-probe electrodes [12, 13] and surface plasmon microscopy [14], it became possible to extend the spatial investigation to

electrocatalytic reactions like the oxidation of hydrogen (H_2), formic acid (HCOOH) and methanol (CH_3OH) or the reduction of peroxodisulfate ($S_2O_8^{2-}$). Detailed experimental and theoretical investigations have shown a vast diversity of patterns [15, 16], ranging from fronts [12-14, 17, 18], standing waves [19], pulses [20, 21] and complex oscillations [22] to various stationary inhomogeneous structures [23, 24].

The studies of electrochemical wave propagation can improve the understanding of activation waves in nerve axons or coupled neurons. This statement actually brings us back to the beginning of studies on nonlinear electrochemical behaviors, which were motivated mainly by the similarity between the propagation of activity in electrochemical systems and nerve impulse propagation [5, 6, 21, 25-27]. Typical propagation velocities in these two types of systems are much faster than for example in chemical (*i.e.*, reaction-diffusion) systems in which concentration waves occur. A peculiarity in electrochemical systems is the nonlocality of the spatial coupling, which is linked to the electric field inside the bulk electrolyte. Concerning nerve impulse propagation, its principle features could be successfully described by the Hodgkin-Huxley theory [28], which incorporates a reaction diffusion system and thus local coupling. As will be discussed in this thesis, these inhomogeneous potential structures can be understood through a combination of nonlinear chemical reactions at the electrode and spatial coupling *via* ion migration.

1.2 General kinetic description of the electrochemical interface

1.2.1 Electrical double layer

When a potential is applied to an electrode, the charges, which accumulate on the electrode surface, attract ions of the opposite charge from the electrolyte. If we consider a metal electrode and an aqueous electrolyte (solution), then we expect to have the charges on the metal side balanced by an equal number of charges in a region adjacent to the electrode in the solution. The simple model of the solution region is that of two planes of charges at a fixed distance from the electrode surface. These layers of charge are then considered to comprise the double layer, shown in Figure 1.1. The solution side of the double layer which is the closest to the electrode, the inner layer, contains solvent molecules and sometimes other species (ions or molecules) that are said to be specifically adsorbed due to

van der Waals type interaction. This inner layer is also called the compact, Helmholtz, or Stern layer. The locus of the electrical center of the specifically adsorbed ions is called the *Inner Helmholtz Plane* (IHP). The next plane towards the solution is defined by the center of the closest solvated ions and called *Outer Helmholtz Plane* (OHP). The interaction of the solvated ions with the charged metal involves only long-range electrostatic forces, so that their interaction is essentially independent of the chemical properties of the ions. The three-dimensional (volumetric) region between the compact layer up to the point where the ionic distribution is no longer influenced by the presence of the metal is called diffuse layer. To probe the double layer potential at the working electrode (WE), that is the potential drop across both the compact and diffuse layer, a secondary electrode has to be used. As the absolute electrode potential cannot be measured, only the difference between the double layer potential of the WE and a reference electrode (RE) can be experimentally accessed.

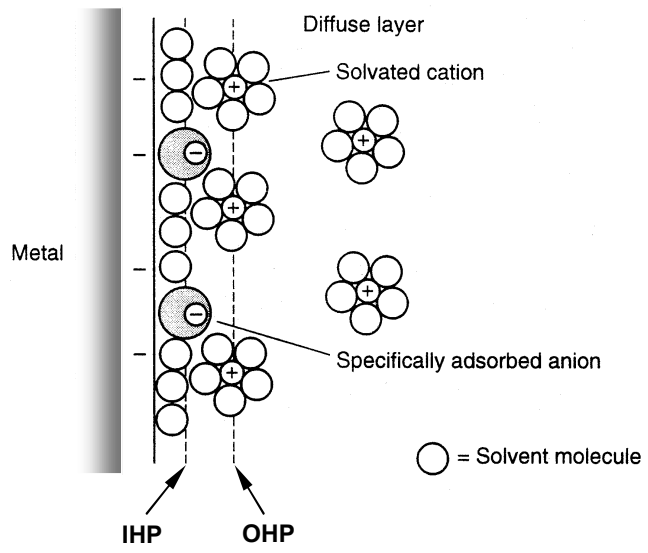

Figure 1.1. Schematic representation of the structure of double layer at a metal electrode. (IHP: Inner Helmholtz Plane, OHP: Outer Helmholtz Plane).

The potential distribution between the WE and the counter electrode (CE) is shown in Figure 1.2. If we set the potential at the CE to zero, the entire potential (Φ_m: metal potential) between the WE and the CE consists of double layer potential (u) and potential

drop in electrolyte Φ_0. On the other hand, Φ_m can be expressed as the sum of the WE potential E_0 with respect to the RE (outer potential) and the RE potential Φ_{RE} :

$$\Phi_m = u + \Phi_0 = E_0 + \Phi_{RE} \tag{1.1}$$

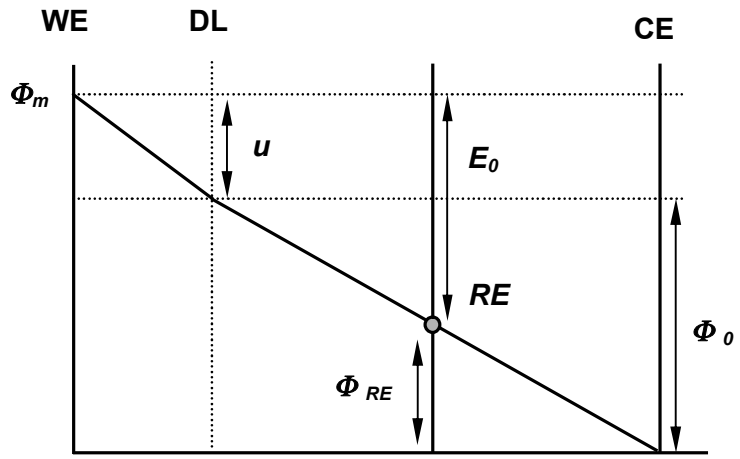

Figure 1.2. Potential profile with the distance between the WE and the CE (DL: double layer).

1.2.2 Dynamical instabilities at electrochemical interface

(A) Negative differential resistance (NDR)

Most electrochemical instabilities are associated with an N-shaped dependence of the current on the electrode potential. In fact, an N-type NDR forms very easily, and its abundant occurrence is also the reason why oscillations are so frequently encountered in electrochemical systems. The possible origins for an N-NDR were discussed in a concise way by Koper and we follow essentially the argumentation from ref. [29]. Generally, the reaction current can be expressed as

$$I_{reac}(u) = nFA(u)\, c(u)\, k(u) \tag{1.2}$$

where n is the number of electrons involved in the charge-transfer process, F Faraday's constant, A the available electrode area, k the rate constant, and c the concentration of the reacting species at the electrode (*i.e.*, at the location of the reaction), the faradaic impedance Z_F is given by

$$Z_F^{-1} = \frac{dI_{reac}(u)}{du} = nF\left(ck\frac{dA}{du} + Ac\frac{dk}{du} + Ak\frac{dc}{du}\right). \qquad (1.3)$$

From Eq. (1.3) it follows that there are three possible origins for negative impedance: (i) the possibility that the available surface area becomes potential-dependent, *e.g.*, due to fast adsorption process ($dA/du < 0$), (ii) potential-dependent adsorption and desorption of a catalyst ($dk/du < 0$), and (iii) Frumkin effect in the double layer ($dc/du < 0$).

(B) Origin of electrochemical bistable and oscillatory behavior

The origin of bistability and oscillations in electrochemical systems is schematically shown in Figure 1.3. Electrochemical dynamics is generally described by the current balance between reaction characteristics of interfacial processes (I_{reac}), capacitive currents for charging the electrochemical double layer (I_{cap}) and the total migration current (I_{mig}) according to

$$I_{cap} + I_{reac} = I_{mig} \qquad \text{or} \qquad C_{dl}\frac{\partial u}{\partial t} = -I_{reac}(u) + I_{mig}(u) \qquad (1.4)$$

where u is the space- and time-dependent interfacial potential (double layer potential) and C_{dl} the interfacial capacity. Steady states are generally governed by the stationary current balance between $I_{reac}(u)$ and the current-voltage reaction of the external circuit (load line in Figure 1.3) obtained by setting the left hand side of Eq. (1.4) to zero.

Assuming a linear potential drop inside the electrolyte under potentiostatic control, the load relation is given by $I = I_{mig} = E_0/R - u/R$ where E_0 is the applied constant potential and R denotes the uncompensated ohmic resistance. As long as the polarization curve $I_{reac}(u)$ is a monotonic function of the double layer potential in Figure 1.3(a), there is only

one steady state for all values of E_0 and R. In contrast, if I_{reac} exhibits a potential region of negative slope, in Figure 1.3(b) and (c), there are values of u and R for which the dynamics exhibits two stable states on branches of positive slope and one unstable state on the middle branch (bistability in Figure 1.3(c)). Because the slope of the polarization curve is related to the sign of the electrochemical impedance, it follows that a negative impedance characteristic (negative differential resistance, NDR) in combination with a sufficiently large ohmic resistance R are necessary for temporal bistability [22, 30]. For spontaneous potentiostatic oscillations of I and u to occur (constant applied potential E_0), an additional essential dynamic variable has to be considered aside from the double layer potential u.

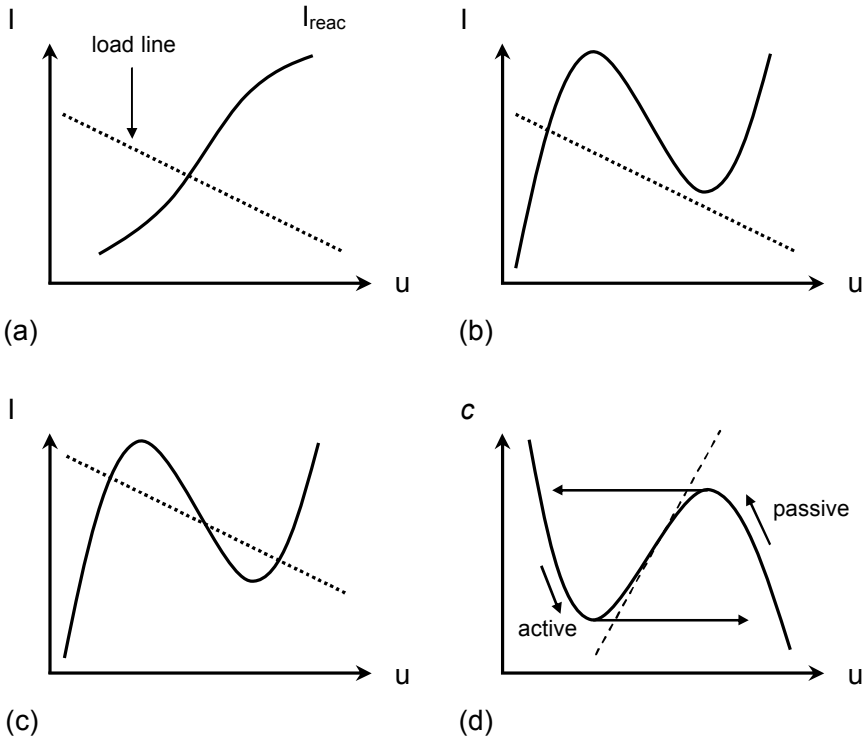

Figure 1.3. Schematic illustration of the origin of electrochemical instabilities: (a) single stationary state (monostability) with load line $I = E_0/R - u/R$ and monotonous faradaic I-u profile; (b) single stationary state with N-shaped faradaic characteristic; (c) three stationary states (bistability) at suitable values of E_0 and R; and (d) relaxation oscillations in a two-variable system. The arrows indicate the trajectory of the periodic orbit within the c~u phase space.

In the simplest case, the volume concentration *c* of a reactive chemical species near the interface can be taken into account resulting in an additional mass balance equation for *c*. Unlike the electrical variables, *c* is generally a slowly changing variable governed by the mass transfer from the bulk and the faradaic process consuming *c*. Figure 1.3(d) sketches out the phase space representation of a periodic orbit; the N-shaped curve and the straight line represent the stationary *c*-*u* values of the charge balance and the mass balance, respectively. Again, the steady state marked by the intersection on the branch of negative impedance is unstable driving the system to relax on the N-shaped manifold. If the system is on the active branch of low values of *u* (high faradaic currents), the faradaic processes gradually consume *c*, and the operation point moves along the N-shaped curve toward smaller *c*. As the system reaches the extreme of the N-shaped curve, the system cannot help but relax to the passive branch (low faradaic current). As *u* is a very fast variable, this relaxation occurs very rapidly. The small current implies low rates of faradic processes allowing *c* to replenish by diffusion. This, in turn, moves the system up along the N-shaped curve in Figure 1.3(c) until it relaxes back to its initial state concluding a periodic cycle. One can show that it is (1) the negative impedance, (2) a sufficiently large ohmic resistance, and (3) a properly balanced difference in time scales between electrical and chemical variables that is crucial for the occurrence of spontaneous potentiostatic oscillations of the type outlined. Such a system will, under galvanostatic conditions, result in bistability, but not exhibit oscillations.

As mentioned above the physicochemical origin of negative impedance can be manifold (Frumkin-type double layer effects, the fast electrosorption of catalytically active or poisoning surface species). In these electrochemical oscillators, the negative impedance is visible by an N-shaped *I*-*u* polarization curve with the Hopf bifurcation located on the middle branch of negative slope. Due to their simple mechanistic requirements, the outlined potentiostatic oscillations have been observed in a large number of experimental systems such as oxidation of cations, reduction of anions, and electrocrystallization [3, 30].

In the context of electro-oxidation of small organic molecules, another mechanistic class of NDR-related electrochemical oscillators is of primary interest. Because its formal kinetic representation allows for a number of different chemical realizations, the current type of oscillator is to be characterized in the form that best matches the electrocatalytic

system under discussion. First, a dominant faradaic process (current providing reaction) is involved that contributes the major portion of the total faradaic charge transfer. Being electrocatalytic, the current-providing reaction typically requires a number of free active surface sites to occur. In the presence of fast electrosorbing surface species reducing the number of free surface sites, say, for large u, the resulting $I_{reac}(u)$ characteristic will exhibit a potential region of negative impedance on an anodic potential scan. Finally, if an additional electrosorbing surface species adds to the mechanism, which is not consumed by the dominant faradaic process, and which adsorbs at small u, but desorbs at large u, then the overall system is able to exhibit both potentiostatic and galvanostatic oscillations for suitable values of the kinetic parameters. Although the chemical requirements necessary for oscillations seem demanding here, a surprisingly large number of oscillations of this type are known, most prominently the electro-oxidations of small organic molecules such as formic acid.

In contrast to the oscillators outlined previously, the Hopf bifurcation is located on an I-u branch with positive slope, that is, the NDR crucial for the instability is not visible on the slow time-scale of the polarization curve. Hence, the NDR is hidden, and according to this distinctive feature, these systems are referred to as hidden negative differential resistance (HNDR) oscillators [15, 30]. Impedance spectroscopy is a common tool to investigate the kinetics of electrochemical processes over a large range of time scales. This makes it an ideal predictive technique to probe electrochemical systems for their capability to exhibit dynamical instabilities [30].

1.3 Spatiotemporal description of the electrochemical interface

It is well known that chemical instabilities may lead to spectacular spatiotemporal phenomena, such as spiral waves, chemical turbulence etc [31]. These patterns result from the coupling of autocatalytic reactions and diffusion. In electrochemical systems, the situation is different, as potential gradients that lead to migration of charged species play an important role. Electrochemical spatial patterns involve the emergence of self-organized, inhomogeneous spatial distributions of the interfacial potential u along the electrode surface. Frequently, potential patterns are also accompanied by spatial variations of concentrations of surface species or volume species near the interface. Dynamical patterns with

inhomogeneous potential distributions require some type of spatial communication or coupling across the electrode surface. Depending on their range, various types of coupling can be distinguished, namely short-range or local coupling, that is, when local perturbations only affect their immediate neighborhood, and global coupling, when local perturbations affect the entire spatial system with equal strength. In addition, the term nonlocal coupling has been coined for situations between the former two, that is, where the coupling between two points is long-range, but decreases in strength. Typical examples of local couplings in chemistry or surface catalysis involve heat and mass coupling by diffusion [32, 33].

The dominant coupling mechanism along electrochemical interfaces is electromigration, that is, the propagation of ions under the influence of a potential gradient. Generally, migration, just like diffusion, seeks to smooth out gradients (at least locally) and therefore exerts a positive coupling between surface locations. In contrast to diffusion, however the effect of electromigration extends over a larger distance resulting in nonlocal coupling [12].

1.3.1 Integral formalism for reaction-migration systems

Here a brief summary of the general treatment of the theory of electrochemical processes is given, as developed by Christoph [34, 35]. According to potential theory, the potential $\Phi(x, z, t)$ inside a volume is given by the charges present, *e.g.*, $\Phi_z(x, t) \equiv \partial\Phi/\partial z(x, z)|_{z=+0}$ in the case of Neumann boundary conditions (Here x donates the spatial coordinate parallel, z the one perpendicular to the boundary). For an electrode in contact with an electrolyte (inside which no net charges exist, *i.e.*, $\Delta\Phi(x, z, t) \equiv 0$), the potential distribution in the electrolyte can thus be expressed in terms of the boundary condition at the electrode

$$\Phi\ (x,z,t) = \int_{el.} G(x,x',z)\Phi_z(x',t)\,dx' \qquad (1.5)$$

where G represents a Green's function, and the integral is taken over the whole electrode. In particular, the potential at the electrode $\Phi_0(x, t) \equiv \partial\Phi/\partial z(x, z)|_{z=+0}$ results in

$$\Phi_0(x,t) = \int_{el.} G_0(x,x')\Phi_z(x',t)\,dx' \tag{1.6}$$

with $G_0(x,x') = \lim_{z\to+0} G_0(x,x',z)$.

The Green's function G can be computed from Coulomb's law

$$\Phi_0(x,t) = \int_{el.} \frac{\sigma(x',t)}{|x-x'|}\,dx' \tag{1.7}$$

and the static field equation, *i.e.*, the fact that the field $\Phi_z(x, t)$ is proportional to the surface charge density $\sigma(x, t)$

$$\Phi_z(x,t) \equiv -2\pi\sigma(x,t). \tag{1.8}$$

Combining Eq. (1.7) and (1.8) results in

$$\Phi_0(x,t) = -\frac{1}{2\pi}\int_{el.} \frac{\Phi_z(x',t)}{|x-x'|}\,dx'. \tag{1.9}$$

Note that the solution to Eq. (1.9) depends crucially on the boundaries of the integral, in physical terms on the geometry of the electrode. Consequently, there is no general solution; rather the integral has to be evaluated for each geometry separately. While the solution is not always analytical, potential theory guarantees that a unique solution exists, which can, if everything else fails, always be approximated numerically.

At an electrode-electrolyte interface an electrical double layer of capacitance C forms. The potential drop across this double layer is given by

$$u(x,t) \equiv u(x,t) = \Phi_m(t) - \Phi_0(x,t). \tag{1.10}$$

Here $\Phi_m(t)$ denotes the (space-independent) potential of the (metal) electrode. If an electrochemical reaction takes place, the neutrality condition in a volume element adjacent to the electrode requires that the capacitive current $C(\partial u(x, t)/\partial t)$ and the faradaic current $i_{reac} = u(x, t)$ are balanced by the migration current $i_{mig} = -\kappa\, \Phi(x, t)$ (κ is the conductivity of the electrolyte):

$$C\frac{\partial u(x,t)}{\partial t} = -i_{reac}u(x,t) - \kappa\Phi_z(x,t). \tag{1.11}$$

Equation (1.11) can be put into integrable form by substituting $\Phi_z(x, t)$ using Eq. (1.6). We invert G_0 to $H_0 \equiv G_0^{-1}$ to obtain

$$\Phi_z(x,t) = -h(x)\Phi_0(x,t) + \int_{el.} H_0(x,x')(\Phi_0(x',t) - \Phi_0(x,t))\, dx' \tag{1.12}$$

with $h(x) = -\int H_0(x,x')dx'$.

Equation (1.12) is now inserted into the evolution equation Eq. (1.11) and Eq. (1.10) is used resulting in

$$\begin{aligned} C\frac{\partial u(x,t)}{\partial t} &= -i_r(u(x,t)) + \kappa h(x)(\Phi_m(t) - u(x,t)) \\ &\quad + \kappa\int_{el} H_0(x,x')(u(x',t) - u(x,t))\, dx' \end{aligned} \tag{1.13}$$

where the spatial coupling is entirely taken care of by the integral expression containing the coupling function $H_0(x, x')$ and the potential difference of two points $u(x', t) - u(x, t)$ considered. $h(x)$ indicates all local chemical dynamics, and $H_0(x, x')$ represents the coupling between two positions x and x'. We refer to the integrodifferential equation Eq. (1.13) as the general reaction-migration equation (RME) in integral form; it is the central equation for the theoretical treatment of reaction-migration system, *i.e.*, electrochemical process.

1.3.2 Coupling function on a ring electrode

As an example of a coupling function, we treat here a ring electrode (following [34, 35]). The case of a ribbon electrode, relevant for chapter 5 will be described there. As already pointed out, the local term $h(x)$ and the coupling function $H_0(x, x')$ have to be calculated for each geometry of the electrode. Here we restrict ourselves to a specific, relatively simple, case; assume a thin annulus of outer radius unity as WE, a pointlike RE located above the center of the annulus at a distance β, and a CE at infinity (the shape of the CE, therefore, becomes irrelevant). Since the WE is assumed thin, it can be treated as one-dimensional, *i.e.*, the radial dependence is neglected, and the spatial coordinate x refers to the angle only. Because of symmetry, all points x of such a WE are equivalent, so that Eq. (1.13) reduces to a space-independent local part (reaction part) and a coupling term which only depends on the distance $|x - x'|$

$$C\frac{\partial u(x,t)}{\partial t} = -i_r(u(x,t)) + \kappa h(x)(\Phi_m(t) - u(x,t)) + \kappa\int_0^1 H_0(|x-x'|)(u(x',t)-u(x,t))\,dx' \quad . \tag{1.14}$$

The electrode potential Φ_m depends on two parameters, namely the distance β between RE and WE and the external resistance R_g of circuit. We combine these into a single parameter B

$$B = R_g\pi\kappa(1-A^2) - \sqrt{1-\beta^2} + \sqrt{A^2+\beta^2} \tag{1.15}$$

For constant applied external potential E_0, the metal potential Φ_m becomes $\Phi_m(t) = (E_0 + hB(u))/(1+hB)$, the total resistance $R = (1+hB)/\kappa h$, so that Eq. (1.14) can be rewritten as

$$C\frac{\partial u(x,t)}{\partial t} = -i_r(u(x,t)) + \frac{E_0 - u(x,t)}{R} + \kappa\int_0^1 H_B(|x-x'|)(u(x',t)-u(x,t))\,dx' \tag{1.16a}$$

$$\text{with } H_B(|x-x'|) = H_0(|x-x'|) + \frac{h^2 B}{1+hB}. \tag{1.16b}$$

For the present geometry, $H_0|x - x'|$ was computed numerically. As is evident from Eq. (1.16b), the complete coupling function $H_B|x - x'|$ includes a space-independent offset, which is determined by the parameter B. Note that for sufficiently negative B, the coupling function becomes negative for increasing $|x - x'|$. Negative coupling ($B < 0$) occurs only for very small (or vanishing) external resistance R_g and small distance β. Conversely, a sufficiently large external resistance and/or large distance between the RE and the WE give rise to a coupling function, and favors synchronization of the dynamical behavior of the electrode.

The limit of infinite B corresponds to the galvanostatic mode of operation (i_g = constant), which is described by

$$E_0 = R\, i_g, \quad H_{B\to\infty} = H_0(|x-x'|) + h \tag{1.17a}$$

$$\begin{aligned} C\frac{\partial u(x,t)}{\partial t} &= -i_r(u(x,t)) + i_g \\ &\quad + \kappa\int_0^1 (H_0(|x-x'|) + h)(u(x',t) - u(x,t))\, dx' \end{aligned} \tag{1.17b}$$

with the total migration current (i_{mig}) = i_g. Note that in this case the space-independent part of the coupling function is positive and at its maximum possible value h, *i.e.*, galvanostatic operation tends to synchronize the dynamical behavior of the whole electrode.

Figure 1.4 shows the coupling function H_B for a thin ring electrode of unitary circumference for two different geometries together with the coupling function. The synchronizing nature of the migration coupling mentioned above becomes apparent when considering the positive offset (solid line), in other words, as H_B is positive everywhere, the spatial coupling is synchronizing. The non-local feature of the migration coupling is also easily seen; in contrast to diffusion, migration couples all elements of the electrode with

each other, though with different strength. The next case (dashed line), denotes a situation in which the RE is placed between the CE and the WE. Here the nature of the desynchronizing negative global coupling is straightforward. There is a negative offset of the coupling function; adjacent points along the ring remain positively coupled, whereas opposite points are negatively coupled. As discussed earlier, this desynchronizing coupling is termed global since it acts along the entire WE, and the negative shift in the coupling function does not depend on the position.

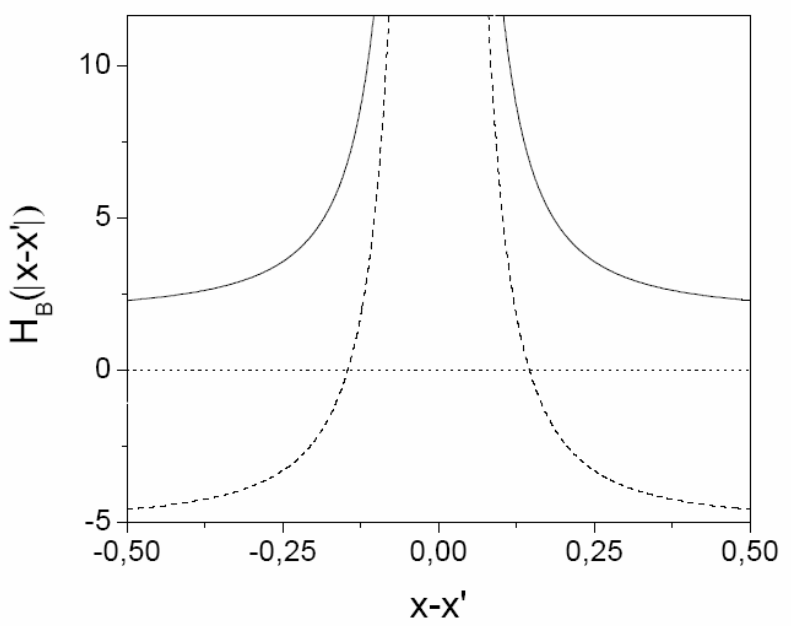

Figure 1.4. Coupling function H_B of thin ring electrode. For small distance of the RE from the WE, H_B is lowered by negative global offset; negative global coupling ($B < 0$, dash line). For large distance of the RE from the WE or additional external resistance till galvanostatic limit, H_B represents strong positive global coupling ($B = \infty$, solid line) from [34].

1.4 Electrochemical formic acid (HCOOH) oxidation

1.4.1 Mechanism of the HCOOH system

Electrochemical oxidation of small organic molecules has been studied for decades because of their high energy density and potential application to fuel cells. It is well known that the oxidation of formic acid has fewer oxidation steps and can be considered as a

model of other small organic molecules. Most studies agree on the fact that formic acid oxidation proceeds *via* a dual path mechanism first proposed by Capon and Parsons [36, 37]. According to these authors, the initial adsorption of formic acid is followed by the formation of a reactive intermediate (presumably ·COOH) which is immediately oxidized further to CO_2, the final product. The reaction steps can be formulated as

$$HCOOH_{(aq)} \rightleftarrows HCOOH_{ad} \tag{1.18}$$

$$HCOOH_{ad} \rightarrow COOH_{ad} + H^+ + e^- \tag{1.19}$$

$$COOH_{ad} \rightarrow CO_2 + H^+ + e^- \tag{1.20}$$

hereby assuming the oxidation of hydrogen radicals to be very fast. The rate of reaction (1.19) is certainly lower than that of reaction (1.20) since radical species are involved, but may be of comparable size to the adsorption reaction (1.18) depending on the diffusion layer thickness, the concentration of HCOOH and the number of available free surface sites. The reaction path given by reaction (1.19) and (1.20) is usually referred to as the direct path of formic acid oxidation. It is important to note that it is this reaction path which provides the necessary current density to account for the measured current peaks.

The dual path mechanism [36, 37] furthermore postulates a parallel reaction path to CO_2 *via* an intermediate which blocks the surface and impedes further adsorption of HCOOH. The nature of this poisoning species has long been the subject of intensive speculation [38-43]. In-situ IR spectrometry, however, showed that the dominating poisoning species is CO [38, 43-45]. The poisoning reaction is assumed to follow the simple scheme

$$HCOOH_{ad} \rightarrow CO_{ad} + H_2O \tag{1.21}$$

At higher potential, CO_{ad} is assumed to be removed through a surface reaction with adsorbed OH stemming from the oxidation of water molecules:

$$H_2O \rightleftarrows OH_{ad} + H^+ + e^- \tag{1.22}$$

$$OH_{ad} + CO_{ad} \rightarrow CO_2 + H^+ + e^- \quad (1.23)$$

Reaction (1.21), (1.22), and (1.23) are referred to as the indirect path of formic acid oxidation. Several authors [46-50] assumed the kinetics of reaction (1.23) to involve an additional free surface site, in order to account for an autocatalytic feedback, but this is clearly not necessary, since autocatalysis is provided *via* potential changes.

1.4.2 Oscillatory instabilities for the HCOOH system

A detailed study of the mechanistic features underlying the dynamical instabilities in HCOOH oxidation was carried out by Strasser *et al.* [51, 52]. These researches comprise systems that exhibit current oscillations on a branch of positive polarization slope. They exhibit potential oscillations under galvanostatic conditions, as well. In their steady-state characteristics the negative impedance of the fast process is hidden by a process on a slower time scale which shows a positive polarization slope. Therefore, these systems are said to have 'hidden' negative impedance and following [15] can be referred to as HNDR oscillators.

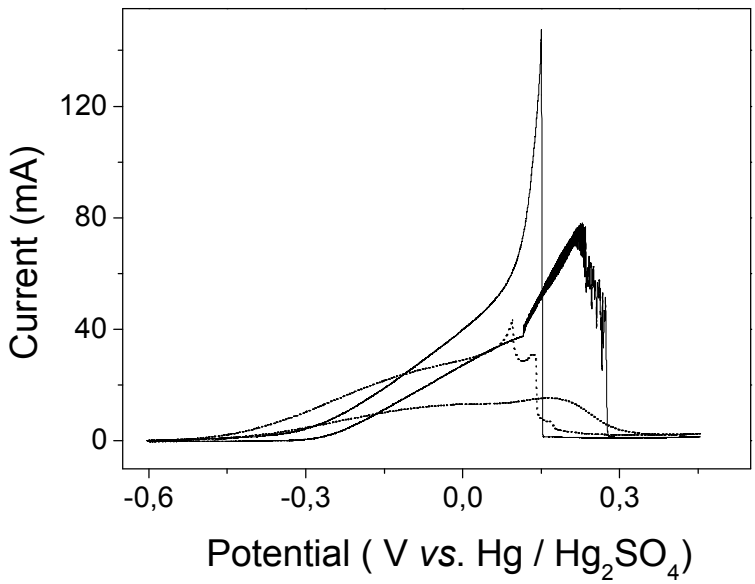

Figure 1.5. Cyclic voltammetry of formic acid oxidation in the absence of Bi^{3+} (dotted line) and in presence of 1×10^{-6} M Bi^{3+} (solid line). After Lee *et al.* [53].

Figure 1.5 shows the effect of Bi adatoms in the formic acid oxidation on a Pt electrode. Dotted line shows the typical CV profile on an unmodified Pt electrode, while about five time higher oxidation current of HCOOH on Bi modified Pt electrode is observed (solid line). This higher electrocatalytic activity of Bi/Pt for HCOOH oxidation can be due to the modification effects of bismuth adatoms such as a third-body effect, the enhanced current may be the result of both steric hindrance of the formation of poisoning species (CO) and intrinsic kinetic enhancement [54-57]. And also, significantly high current oscillations are observed over a broad potential region on Bi modified Pt electrode. It indicates periodic activating and passivating process of the electrode.

1.5 Motivation and outline of this thesis

An important aspect of investigations of pattern formation in chemical systems has always been that these systems can function as models, especially for biological systems. The contribution of such investigations is highly significant for the understanding of biochemical oscillations, cellular rhythms, or the formation of spatial patterns. Early studies on pattern formation in electrochemical systems were motivated by the similarity of potential waves that had been observed for metal dissolution reactions and the propagation of electrical signals in the nervous system [6, 7, 58]. Up to now, a central role has been assigned to the universal aspect of nonlinear phenomena, which establishes the continued interdisciplinary interest on chemical nonequilibrium structures. Electrochemical systems are ideal model systems for a variety of processes of pattern formation, particularly if they involve the interaction of chemical and electrical properties. Such systems are often encountered in biological systems (cell-division, rhythms of cilia, muscle, *e.g.*, heart, and nerve cells).

The aim of this thesis is to explore the spontaneous self-organization phenomena in an electrochemical system. In particular, the present work deals with the experimental investigation of spatiotemporal pattern formation in a self-organizing electrochemical reaction on two shapes of electrode; ribbon and ring electrode. While the ring geometry allows for pattern formation (in azimuthal direction) without edges and maximum symmetry, a ribbon electrode is ideal for the study of edge effects and different environments for electrode patches with different distance from the edges. The symmetry of

a ring can be broken by placing the RE to one side instead of in the middle, or by insulating parts of the ring, hereby introducing edge effects with otherwise unaltered dynamics.

This thesis organized in the following way; after this introduction, the experimental setup is explained and the techniques used for the investigation are presented in chapter 2. Chapter 3 introduces former results about basic pattern formations on a ring electrode in potentiostatic condition, and then concentrates on the transition from periodic potential oscillations to *Shil'nikov* chaotic potential oscillations at fixed current using the Pt ring electrode during the electrochemical oxidation of formic acid with bismuth ions. In chapter 4 spatiotemporal pattern formations on a Pt ring electrode for the effect of an asymmetrically placed reference electrode are investigated in order to experimentally study the effect of the global feedback superimposed by this additional asymmetric effect. In chapter 5, results on the local inhomogeneity and migration coupling caused by the edge effect of a ribbon electrode during the electrochemical oxidation of formic acid with bismuth ions are described and discussed. Chapter 6 deals with same electrolyte but with a partially insulated Pt ring electrode. In particular, we discuss pulses on a Pt ring electrode, which were observed to jump over the insulated areas of the ring with considerably enhanced local velocity. This effect is analogous to *saltatory conduction* in myelinated nerve axons, and can be rationalized in terms of nonlocal migration coupling in the electric field. Finally, the results are summarized in chapter 7.